Paper submitted to NAFEMS World Congress'97
10/01/1997

Hydromechanical Coupling and Strain Localisation.

R. Charlier and J.P. Radu[1]

MSM Department, Université de Liège & ALERT Geomaterials

Abstract
This paper is devoted to the numerical modelling of the strain localisation in a water saturated sample of soil, using a large strain finite element code. First the large strain solid mechanics equations are recalled. An internal friction constitutive law is used. Then the coupling with a pore fluid is considered, and the linkages between the seepage and the soil strain and stress evolution is taken in account through an effective stress postulate and an adaptation of the storage law. Coupled finite elements are developed. Unsaturated media are considered using the Bishop formulation and an adaptation of the seepage model. Finally the developed finite element code is applied to the modelling of the plane strain compression of some sample differing by the pore fluid state. Drained case, undrained fully saturated and undrained partly saturated cases are considered. Two soils, differing by their permeability, are modelled, in order to analyse the seepage effect on the strain localisation availability.

1. INTRODUCTION

Strain localisation has been extensively investigated in metals, in soils and in rocks for about two decades. Mainly drained behaviour has been studied in soils and rocks. However practically most of these materials are fully or partially saturated by water, oil, gas,... The question of the bifurcation to a localised strain mode in a biphasic soil remains quite open. Now it is particularly important, for examples in geotechnics (analysis of landslides, of foundation stability,...) or in tectonophysics (sedimentary basin evolution,...).

[1] MSM Department, Université de Liège, 6 quai Banning, 4000 Liège Belgium, and ALERT Geomaterials

Only very few authors have proposed solution to the strain localisation problems for saturated soils. Desrues and Mokni [3] have experimented the undrained saturated localisation in sand. They performed a series of biaxial compressions (in plane strain state) on Hostun sand in order to characterise the localisation appearance and the shear band mode. Vardoulakis and Han [8, 11, 12] have realised similar experiments on a clay. Loret and Prevost [4] have proposed first some theoretical and numerical analysis of such problems. Schrefler [7] has more recently proposed a finite element modelling of a multiphase localisation problem. But this analysis is limited to small strains problems and is based on dynamic and seepage coupled model.

The present paper is devoted to a finite element modelling of the strain localisation in a (partly) saturated soil sample during a biaxial compression. First the large strain formalism is recalled. A Van Eekelen - Drücker Prager constitutive law is used. The hydromechanical coupling is based on the Terzaghi's postulate and on the storage law. Unsaturated behaviour is then derived as an extension of the previous equations. Monolytical finite element are developed. The achieved code is used to model some biaxial compressions in various states : drained, undrained saturated, undrained unsaturated,... and under different permeabilities.

2. LARGE STRAINS IN SOLID MECHANICS

Strain localisation is generally associated to large strains and large rotations. In the following the mechanical equilibrium is formulated in the current configuration using the Cauchy stresses. The virtual power equation is giving a global equilibrium equation :

$$\int_v \sigma_{ij}\delta\varepsilon_{ij}\,dv = \int_{a_\sigma} t_i\delta u_i\,da \qquad (1)$$

The Jaumann correction is used in order to give an objective stress rate:

$$\dot{\underline{\sigma}} = \tilde{\underline{\sigma}} + \underline{W}\,\underline{\sigma} + \underline{\sigma}\,\underline{W} \qquad (2)$$

where $\underline{W}$ is the antisymmetrical part of the velocity gradient $\underline{L}$:

$$\underline{L} = \frac{\partial \underline{v}}{\partial \underline{x}} = \underline{D} + \underline{W} \qquad (3)$$

An elastoplastic constitutive law is postulated in order to reproduce the classical internal friction soil model which is generally observed on sand. Most authors are using the Drücker-Prager model which associates in its yield surface equation the first and second stress invariant :

$$f = II_{\hat{\sigma}} + mI_\sigma + k$$

$$I_\sigma = \sigma_{ii} \qquad (4)$$

$$II_{\hat{\sigma}} = \sqrt{\frac{1}{2}\hat{\sigma}_{ij}\hat{\sigma}_{ij}}$$

where $\underline{\hat{\sigma}}$ is the stress deviator. The material parameters are related to the friction angle ϕ and to the cohesion c by :

$$m = \frac{2\sin\phi_C}{\sqrt{3}(3-\sin\phi_C)}$$
$$k = \frac{6c\,\cos\phi_C}{\sqrt{3}(3-\sin\phi_C)} \qquad (5)$$

This model can give good results for low internal friction angle materials. However for sands whose friction angle lies between 30° and 45°, the Drücker-Prager model gives poor (and sometimes bad) results. In fact if the model parameters are calibrated on a triaxial friction angle the extension friction angle is much larger. Van Eekelen [10] has proposed an extension of the Drücker Prager model which is based on the Lode angle β. The assumed yield surface is the following :

$$f = II_{\hat{\sigma}} + a(1+b\sin 3\beta)^n (I_\sigma - \frac{3c}{\tan\phi_c}) \qquad (6)$$

$$a,b = fct(\phi_C,\phi_E)$$

A non associated plastic model is formulated using a plastic potential g similar to the yield surface f :

$$g = II_{\hat{\sigma}} + A(1+B\sin 3\beta)^n (I_\sigma - \frac{3c}{\tan\psi_c}) \qquad (7)$$

$$A,B = fct(\psi_C,\psi_E)$$

When a small strain formulation is assumed, the strain decomposition between its elastic and plastic parts is assumed :

$$\underline{\dot{\varepsilon}} = \underline{\dot{\varepsilon}}^e + \underline{\dot{\varepsilon}}^p \qquad (8)$$

In a large strain formulation one often postulates an unloaded configuration, which is leading to a multiplicative decomposition of the elastic and plastic Jacobian matrix :

$$\underline{F} = \underline{F}^p \underline{F}^e \qquad (9)$$

We assume here that the elastic part of the deformation is small compared to the unity. This yields an approximately additive decomposition of the strain rate :

$$\underline{D} = \underline{D}^E + \underline{D}^p \qquad (10)$$

These hypothesis have been discussed by different authors (Sidoroff [7], Mandel [5]).

Here we do not take any hardening into account. Therefore using the equations (4) to (8) and the consistency condition, one obtains easily the stress rate - strain rate equation :

$$\underline{\tilde{\sigma}} = \underline{\underline{C}}^{ep}\,\underline{\dot{\varepsilon}} \qquad (11)$$

On some boundaries, pressures can be applied. It should be mentioned that the imposed forces are following forces. In a large strain formalism they are contributing to the stiffness matrix by a unsymmetrical term.

3. FLOW IN POROUS MEDIA

In a saturated porous medium, flow is assumed to follow the Darcy's law :

$$\underline{v} = -K\underline{\nabla}(\frac{p}{\gamma} + z) \qquad (12)$$

where K is the permeability, p the pore pressure, z the level, γ the fluid specific weight and $\underline{v}$ the Darcy's velocity. If partly saturation is to be considered, the Darcy's law (12) can be used assuming that the permeability K is varying with the saturation degree :

$$K = K(S_r) \qquad (13)$$

We will suppose hereafter that this law is a linear one :

$$K = K_0 S_r \qquad (14)$$

The storage law is giving the evolution of the amount of fluid mass per unit of soil volume:

$$\dot{S} = n\frac{\dot{p}}{\chi_w} \qquad (15)$$

When the fluid saturation degree S_r is varying, a second storage term is necessary :

$$\dot{S} = n\frac{\dot{p}}{\chi_w} + n\dot{S}_r \qquad (16)$$

The balance equation :

$$\underline{\nabla}^T \underline{v} + \dot{S} = 0 \qquad (17)$$

is used and transformed using the virtual power principle in order to formulate finite elements.

When two fluids are partly saturating the pores, two set of equations (12-17) should be written. However if one fluid is a gas, its behaviour can sometimes be neglected, considering that its pressure remains quite constant, what we will do in the following.

On the other hand it is necessary to formulate a retention curve associating the saturation degree and the suction (which is the difference between the non-wetting and the wetting fluid pressures). We here are using an arc tangent relation (figure 1) :

$$S_r = \frac{1}{\pi} arctg \frac{s-\beta}{\alpha} + \frac{1}{2} \qquad (18)$$

$$s = p_{gas} - p_{liquid}$$

When considering a water saturated and dilatant soil under shear loading (e.g. in the hereafter considered biaxial compression) the material tends to dilate but the pore fluid (which is quite incompressible) does not allow that. The fluid pressure therefore decreases from its initial value (generally a back-pressure imposed to ensure the good saturation by dissolving air in water). When the water pressure tends to the atmospheric pressure, the dissolved air appears as bubbles. The fluid is now biphasic, what means that the soil is partly saturated in

air and water. If the initial air content is low enough, a similar desaturation will appear when cavitation will occur. In that case the gas is composed of water vapour bubbles. Whatever the way the soil becomes partly saturated, the fluid compressibility increases quickly at that time. This phenomenon will be simply modelled by using a retention curve postulating a desaturation around the atmospheric pressure (figure 1).

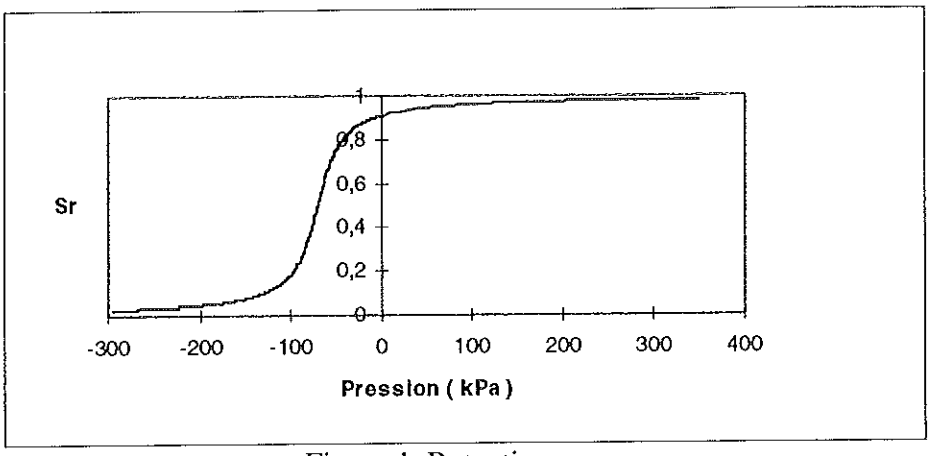

Figure 1. Retention curve

4. HYDROMECHANICAL COUPLING

Stresses are affected by the seepage. This is modelled for saturated media by the Terzaghi's postulate. It is here written in an incremental form:

$$\underline{\tilde{\sigma}} = \underline{\tilde{\sigma}'} - \dot{p}\underline{I} \qquad (19)$$

If the soil is partly saturated by two fluids, this postulate is not more valid. Bishop has proposed a modified form :

$$\underline{\tilde{\sigma}} = \underline{\tilde{\sigma}'} - \chi(S_r)\dot{p}\underline{I} \qquad (20)$$

where $\chi(S_r)$ is a new function to be defined from experimental results. This relation can be analysed as a mixture law (Schrefler [6]). It becomes then :

$$\underline{\tilde{\sigma}} = \underline{\tilde{\sigma}'} - S_r \dot{p}_{liquid}\underline{I} - (1-S_r)\dot{p}_{gas}\underline{I} \qquad (21)$$

If the gas pressure remains near to the zero pressure reference (atmospheric pressure), the last term disappears.

It has been shown (Alonso et al. [1]) that this effective stress postulate gives qualitatively good results for soils mainly shear loaded. However for soils undergoing much isotropic loading (oedometric tests, variation of the suction level,..) it does not well reproduce the experimental results. A CamClay like model has been proposed by Alonso, Gens and Josa [1] for these kind of loading. However this type of model will not be used in the following.

The fluid flow is affected by the soil mechanics through the storage law in which the pores volume is modified according to the volumetric strain rate :

$$\dot{S} = n\frac{\dot{p}}{\chi_w} + n\dot{S}_r + \dot{\varepsilon}_{ii} \qquad (22)$$

In this equation, it is supposed that the soil grains (or the soil squeleton) volume does not change with respect to the mean effective stress variation.

The soil mechanics is involving large strains. This does not affect the fluid flow in the sense that the balance equation is formulated at one instant per time step (generally at the step end). Moreover the storage and Darcy's flow laws are not depending on the history. Therefore no objective correction is needed. On the other hand, the additive strain decomposition (10) is here assumed to remain valid (De Buhan et al. [2]).

5. FINITE ELEMENTS

A plane large strain finite element has been implemented in the finite element code LAGAMINE. It is an isoparametric element with 8 nodes and 4 Gauss integration points. This means that the co-ordinates, velocities and pore pressures are discretised by the same shape functions. The hydromechanical coupling is a monolithical one. The stiffness matrix is tangent in the Newton Raphson sense. It associates 3 dof per node. It can been schematised as follow :

$$d\begin{Bmatrix} F_1 \\ F_2 \\ Q_{liq} \end{Bmatrix} = \begin{bmatrix} m-m & m-m & m-s \\ m-m & m-m & m-s \\ s-m & s-m & s-s \end{bmatrix} \begin{Bmatrix} dx_1 \\ dx_2 \\ dp_w \end{Bmatrix} \qquad (23)$$

Staggered schemes have also been proposed (Zienckiewicz [13]) which allow to obtain solutions for some problems for which the monolithical scheme fails due to opposite time stepping conditions for the mechanical and hydraulical problems. However the monolithical scheme has proved to be efficient for the considered problem.

6. APPLICATION

We consider in the following the biaxial compression which is a classical test for the study of the strain localisation in soils (Mokni and Desrues [3], Vardoulakis [9,11,12]). A parallelepiped sample of soil (figure 2) is under plane strain conditions thanks to 2 rigid glass plates. Two sample sizes are considered : 175 x 350 mm^2 and 164 x 173 mm^2.

A constant pressure is applied to the lateral boundaries. The initial stress state is isotropic. This lateral pressure remains then constant. The lower basis lies on a frictionless plateau ; the upper one is compressed by a second frictionless plateau.

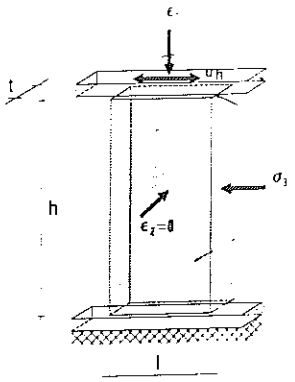

Figure 2. Soil sample under biaxial compression.

6.1. Rectangular sample

The initial stress state is isotropic with σ'_0 = 100 kPa. The sample is discretised by 10 x 20 8-nodes finite elements. The soil is modelled by a elastic - perfectly plastic Drücker-Prager model whose parameters are indicated in table 1. The seepage parameters are given in the same table. The compression velocity (upper plateau) is $\dot{H} = 1{,}8\ 10^{-3}\ mm/s$.

parameter	symbol	value
Young modules	E	26 GPa
Poisson's ratio	ν	0.3
compression friction angle	ϕ_c	25°
dilatancy angle	ψ	10°
water compressibility	χ_w	3. GPa
porosity	n	0.45

table 1 : Rectangular sample - mechanical and seepage parameters.

case number	drainage	saturation	permeability
1	drained	no means	p = 0.
2	undrained	saturated	10^{-20} m/s
3	undrained	saturated	10^{-07} m/s
4	undrained	varying saturation	10^{-20} m/s

table 2 : rectangular sample - various modelled cases.

Some different cases have been modelled (table 2). The first modelling case corresponds to a drained sample. The figure 3 shows the deformed mesh after 5, 10 and 15 % of axial strain (no deformation amplification). A shear band has clearly appeared. Shear strains up to 80% and volumetric strains up to 5%

can be observed inside the band (the peak value is of course depending on the mesh size). This shear banding results is typical from soil shear band modelling.

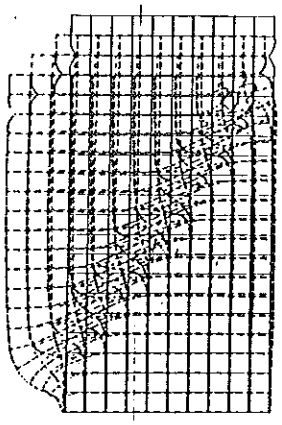

Figure 3. Case 1 : deformed mesh after 5, 10 and 15 % of axial strain (no deformation amplification).

In the case 2, the sample is fully saturated by water and the initial back-pressure is high enough to avoid any cavitation or other de-saturation. The mesh remains rectangular and the stress and pore pressure state is homogeneous during the whole compression process. The global volume remains constant. The volumetric strains are quasi null. The pore pressure variation is Δp = 500 kPa at the end of the simulation.

The case 3 is similar but the permeability is much more larger. The deformed mesh after 5, 10 and 15 % of axial strain (no deformation amplification) is presented at figure 4. Two shear bands have now appeared. The stress and pore pressure state is no more homogeneous. The global volume remains always constant. However the volumetric strains are not homogeneous (figure 5) and varies from about 4% dilatation inside the band to about 1.5% contraction outside it.

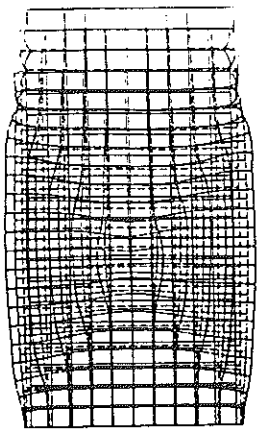

Figure 4. Case 3 : deformed mesh after 5, 10 and 15 % of axial strain (no deformation amplification).

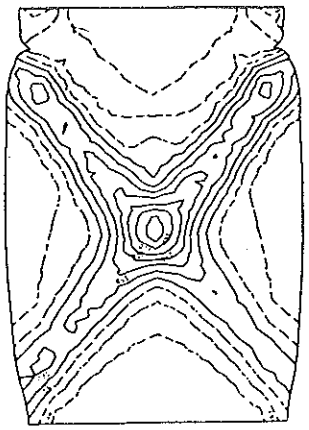

Figure 5. Case 3 : volumetric strains in the deformed mesh after 15 % of axial strain.

According to these variations of the void ratio the water storage and the pore pressure are also varying. It results in pressure gradients and in water flows which are presented on the figure 6. These Darcy's velocities are showing that the two shear bands (figure 4) are not always active together. After 5 % of strain the shear banding is not really clear. After 10 % the two shear bands are slipping together. At the end of the analysis only one band is active.

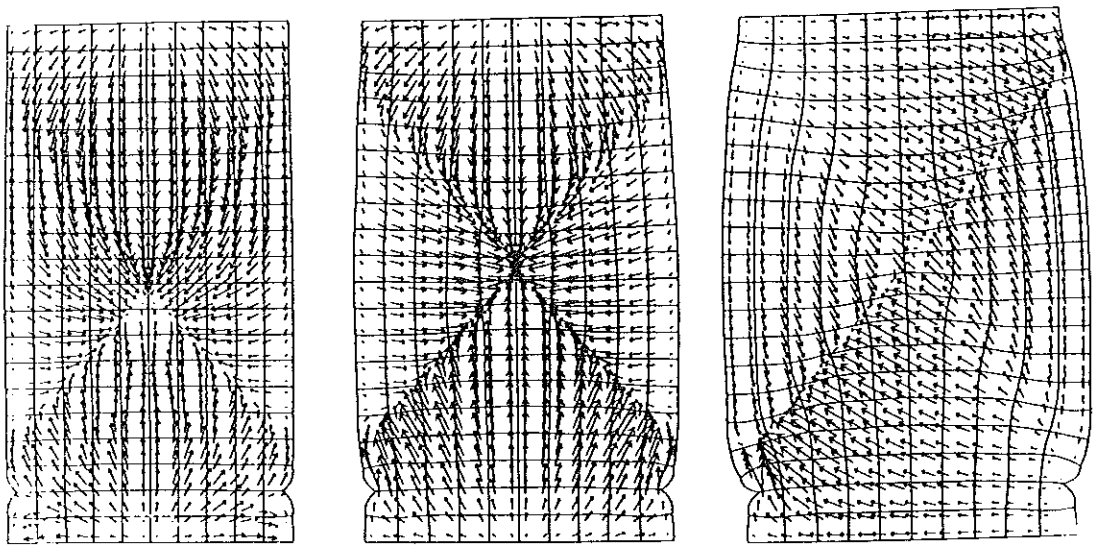

Figure 6. Darcy's velocities in the deformed mesh after 5, 10 and 15 % of axial strain.

The last analysis case (n° 4) is concerned with a unsaturated case. There is no initial back-pressure. Therefore any pore pressure decrease is inducing a de-saturation. Due to the Bishop's effective stress principle, the pore pressure

effect is reduced. Moreover the gas phase is supposed to be under constant pressure, what means that it is highly compressible. This is relaxing in some sense the constant volume condition, which is associated to undrained saturated tests. Therefore we come back to similar results as in the case 1.

6.2. Square sample

The initial stress state is isotropic with σ'_0 = 100 kPa. The sample is discretised by 30 x 30 8-nodes finite elements. The soil is modelled by a elastic - perfectly plastic Van Eekelen model whose parameters are given in table 3. The seepage parameters are indicated in the same table.

parameter	symbol	value
Young modules	E	35 MPa
Poisson's ratio	ν	0.4
compression friction angle	ϕ_c	41°
extension friction angle	ϕ_e	41°
dilatancy angle	ψ	10°
permeability	K	10^{-16}m/s
water compressibility	χ_w	3. GPa
porosity	n	0.3

table 3 : Square sample: mechanical and seepage parameters.

When globally undrained states are considered, the sample is supposed to be inside a impervious membrane. Therefore the total pore fluid mass remains constant. An initial back-pressure p_0 = 30 kPa is applied. The rate of displacement of the upper boundary is V= 1.64 10^{-3}mm/s or 10^{-3} %/s (of the initial height).

Loading has been performed up to 10 % of mean axial deformation. The simulation results are partly given in the figures n° 7, 8 and 9. Their analysis can be summarised as follow. No strain localisation is apparent on the deformed mesh. However the water pore pressure map (figure 7) shows clearly a localisation band where the pore pressure has highly decreased (from 130 kPa initially to -120 kPa after 9% of axial deformation). A little later (10% compression) the localisation scheme has changed (figure 8a) and two localised band have appeared. The lower water pressure is a little lower (-160 kPa). These negative pore pressures are associated to a partial saturation (retention curve - cf. figure 1) At the band centre the saturation degree has decreased to S_r = 0,95. The water pore pressure has decreased because of the band dilatancy. The sample shearing concentrates in the band and it is associated to a local volume increase. Water accommodates this by decreasing its pressure. Due to the resulting pressure gradient water flow from outside the band to inside it (figure 8b).

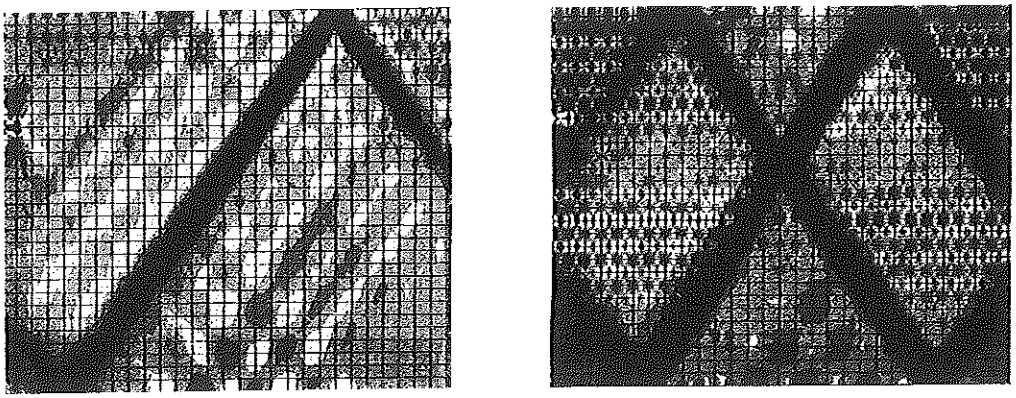

Figure 7. Water pressure after 9 and 10 % compression.

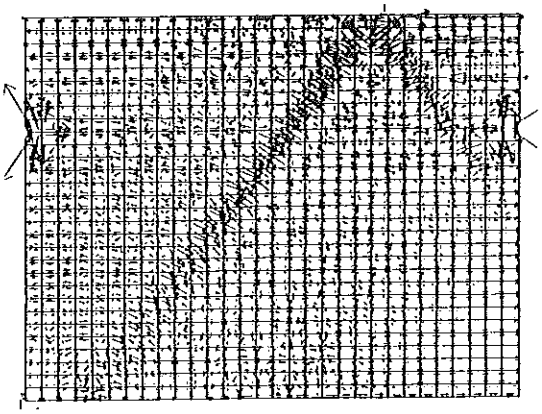

Figure 8. Water flow - Darcy's velocities after 10% compression.

11. CONCLUSIONS

A hydromechanical large strains finite element code has been developed for soils and rocks modelling. It has been applied to the modelling of biaxial compressions on various soil samples.

Pure mechanical analysis (on drained samples) shows clearly a strain localisation. The modelling is possible up to very large strains.

In a saturated soil sample, if the permeability is small enough compared to the loading velocity, water has not enough time to move during any strain localisation process. Then the unsaturated state is a global and a local one. No strain localisation can appear.

In a dilatant sample the pore pressure is continuously decreasing during the stress deviator increase (uniaxial compression phase). When that pressure becomes small enough, gas bubble are appearing due to cavitation in pure water or to the end of air dissolution in other cases. Then the pore fluid becomes a biphasic one with a high compressibility, and a drained like localisation is possible.

If the permeability is larger, then water moves and allows a strain localisation in a dilatant medium. The undrained condition is a global one. This

means that the total volume remains constant due to the low fluid compressibility. However at a local level, dilatancy as well as contractancy are appearing. The volumetric strain integral over the whole sample volume is quite null (with respect to the fluid compressibility).

ACKNOWLEDGEMENTS

The authors are grateful to the *Groupement de Recherche en géomécanique des Roches Profondes,* to the EC through the financial support to the network *ALERT Geomaterials,* and to the FNRS.

REFERENCES

1. E.E. ALONSO, A. GENS and A. JOSA. A constitutive model for partially saturated soils. Géotechnique 40, N° 3, pp. 405-430, 1990.
2. E. BOURGEOIS, P. de BUHAN et L. DORMIEUX. Formulation d'une loi élastoplastique pour un milieu poreux saturé en transformation finie. C.R. Acad.Sci, Paris, t.321, Série IIb, pp. 175-182, 1995.
3. M. MOKNI Relations entre déformations en masse et déformations localiseés dans les matériaux granulaires. Thesis UJF-INPG, Grenoble, 1992.
4. B. LORET, J.H. PREVOST Dynamic strain localization in fluid-saturated porous media. Jl. of Eng. Mech. Vol. 117, N° 4, pp. 907-922, avril 1991.
5. J. MANDEL Relations de comportement des milieux élastoplastiques et élasto-visco-plastiques - Notion de repère directeur. Foundations of plasticity, Ed. A. Sawczuk, Noordhoff (1973).
6. B.A. SCHREFLER, L. SIMONI, X.K. LI, O.C. ZIENKIEWICZ. Mechanics of partially saturated porous media. Numerical Methods and Constitutive Modelling in Geomechanics. C.S. Desai and G. Gioda, ed., CISM Courses and Lectures, N° 311, Springer Verlag, 169-209, 1990.
7. B.A. SCHREFLER, L. SANAVIA and C.E. MAJORANA. A multiphase medium model for localisation and postlocalisation simulation in geomaterials. Mechanics of Cohesive Frictional Materials, Vol. 1, 95-114 (1996).
8. F. SIDOROFF. Cours sur les grandes déformations. CNRS, Rapport GRECO Grandes déformations, N° 51, Sophia Antipolis, 1982.
9. C. HAN and I.G. VARDOULAKIS. Plane strain compression experiments on water-saturated fine-grained sand. Géotechnique 41, N° 1, pp. 49-78, 1991.
10. H.A.M. van EEKELEN. Isotropic yield surfaces in three dimensions for use in soil mechanics. Int. Jl. for Numerical and Analytical Methods in Geomech., Vol.4, 89-101, 1980.
11. I.G. VARDOULAKIS. Deformation of water-saturated sand: I. Uniform undrained deformation and shear banding. Géotechnique, 46, n° 3, 441-456, 1995.
12. I.G. VARDOULAKIS. Deformation of water-saturated sand: II. The effect of pore water flow and shear banding. Géotechnique, 46, n° 3, 457-472, 1995.
13. O.C. ZIENKIEWICZ, D.K. PAUL, A.H.C. CHAN. Unconditionally stable staggered solution procedure for soil-pore fluid interaction problems. Int. Jl. for Numerical Methods in Engineering. Vol. 26, 1039-1055, 1988.